Dalton Transactions

ROYAL SOCIETY OF CHEMISTRY

PAPER

View Article Online
View Journal | View Issue

Check for updates

Cite this: *Dalton Trans.*, 2025, **54**, 12463

High-spin face-capped deltahedra in divanadadicarbaboranes are very different from the singlet structures of chromium analogues†

Horaţiu Casian,[a] Alexandru Lupan *[a] and R. Bruce King *[b]

Received 27th June 2025,
Accepted 16th July 2025

DOI: 10.1039/d5dt01520k

rsc.li/dalton

Using density functional theory (DFT), divanadadicarbaboranes $Cp_2V_2C_2B_{n-4}H_{n-2}$ are found to have very different low-energy structures than the corresponding dichromadicarbaboranes $Cp_2Cr_2C_2B_{n-4}H_{n-2}$. Thus, the low-energy divanadadicarbaborane structures with n vertices have triplet or quintet states rather than singlet spin states, frequently based on an $(n-1)$-vertex VC_2B_{n-4} deltahedron having a face capped by the second vanadium atom bearing most of the spin density. Such structures are analogous to the low-energy structures of dimanganaboranes $Cp_2Mn_2B_{n-2}H_{n-2}$, even though the vanadium and manganese systems are not isoelectronic with each other. Most of the low-energy 8-vertex $Cp_2V_2C_2B_4H_6$ structures are based on the hexagonal bipyramid, whereas most of the low-energy 9- and 10-vertex structures are based on the 9-vertex iso*closo* deltahedron. The bicapped square antiprism capped by a high-spin vanadium vertex is characteristic of the low-energy 11-vertex $Cp_2V_2C_2B_7H_9$ structures. Similarly, an 11-vertex *closo* deltahedron capped by a high-spin vanadium vertex is the lowest energy $Cp_2V_2C_2B_8H_{10}$ structure by a substantial margin of ~18 kcal mol^{-1}.

1. Introduction

The preferred structures of deltahedral boranes and isoelectronic carboranes are based on the most spherical *closo* deltahedra in which all of the faces are triangles and the vertices are as nearly similar as possible (Fig. 1).[1–3] Each of the boron and carbon vertices in such structures uses one valence orbital for bonding to an external atom or group R such as hydrogen, a halogen, or a simple alkyl or aryl group. This leaves the remaining three vertex atom valence orbitals available to participate in skeletal bonding. Much of the early development of this chemistry was based on structures with an external hydrogen atom bonded to each boron or carbon vertex. In the electron bookkeeping for such systems, each BH vertex thus contributes two skeletal electrons and each CH vertex contributes three skeletal electrons. The preferred n-vertex deltahedral species were of the $B_nH_n^{2-}$, $CB_{n-1}H_n^-$, and $C_2B_{n-2}H_n$ types with $2n + 2$ skeletal electrons as discussed by Wade and Mingos[4–6] in early papers and justified by chemical bonding models based on graph theory/topology[7] and tensor surface harmonics.[8]

The research groups of Hawthorne[9] and Grimes[10] were the pioneers in synthesizing the first deltahedral boranes having transition metal vertices. Vertices of the CpM type (Cp = η-C_5H_5) were preferred owing to the robust nature of the cyclopentadienyl–metal bond. This allows a variety of chemical transformations to be performed on the metallaborane structure with the CpM vertices remaining intact. Cobalt vertices of the CpCo type were used in the early metallaborane and metallacarbaborane research. For electron bookkeeping purposes, a CpCo vertex is isoelectronic with a BH vertex as a contributor of two skeletal electrons. Thus, among the nine valence orbitals of the sp^3d^5 manifold of the cobalt atom, three are used for external bonding to the Cp^- anion and three are occupied by lone pairs. This leaves three orbitals and two electrons available for skeletal bonding, corresponding to the favored 18-electron configuration for the cobalt atom.[11–13] In the early work, Hawthorne's group[9] focused on metallaboranes obtainable using $B_{10}H_{14}$ as the boron hydride source, whereas Grimes' group[10] focused on metallaboranes obtainable from B_5H_9. Because of the U. S. government's interest in the 1960s in the use of boron hydrides as possible rocket fuels, these key binary boron hydride starting materials were much more readily available then than they are now in modern times.

The pioneering work by Hawthorne and Grimes on metallaboranes was followed by work in the laboratory of Kennedy on

[a]*Faculty of Chemistry and Chemical Engineering, Babeş-Bolyai University, Cluj-Napoca, Romania. E-mail: alexandru.lupan@ubbcluj.ro*
[b]*Department of Chemistry and Center for Computational Quantum Chemistry, The University of Georgia, Athens, GA, USA. E-mail: rbking@uga.edu*

†Electronic supplementary information (ESI) available: Initial structures, distance and energy ranking tables, orbital energies and HOMO/LUMO gaps, complete Gaussian09 reference (.pdf file), and the concatenated .xyz file containing the optimized structures that can be visualized using free software such as the Mercury program. See DOI: https://doi.org/10.1039/d5dt01520k

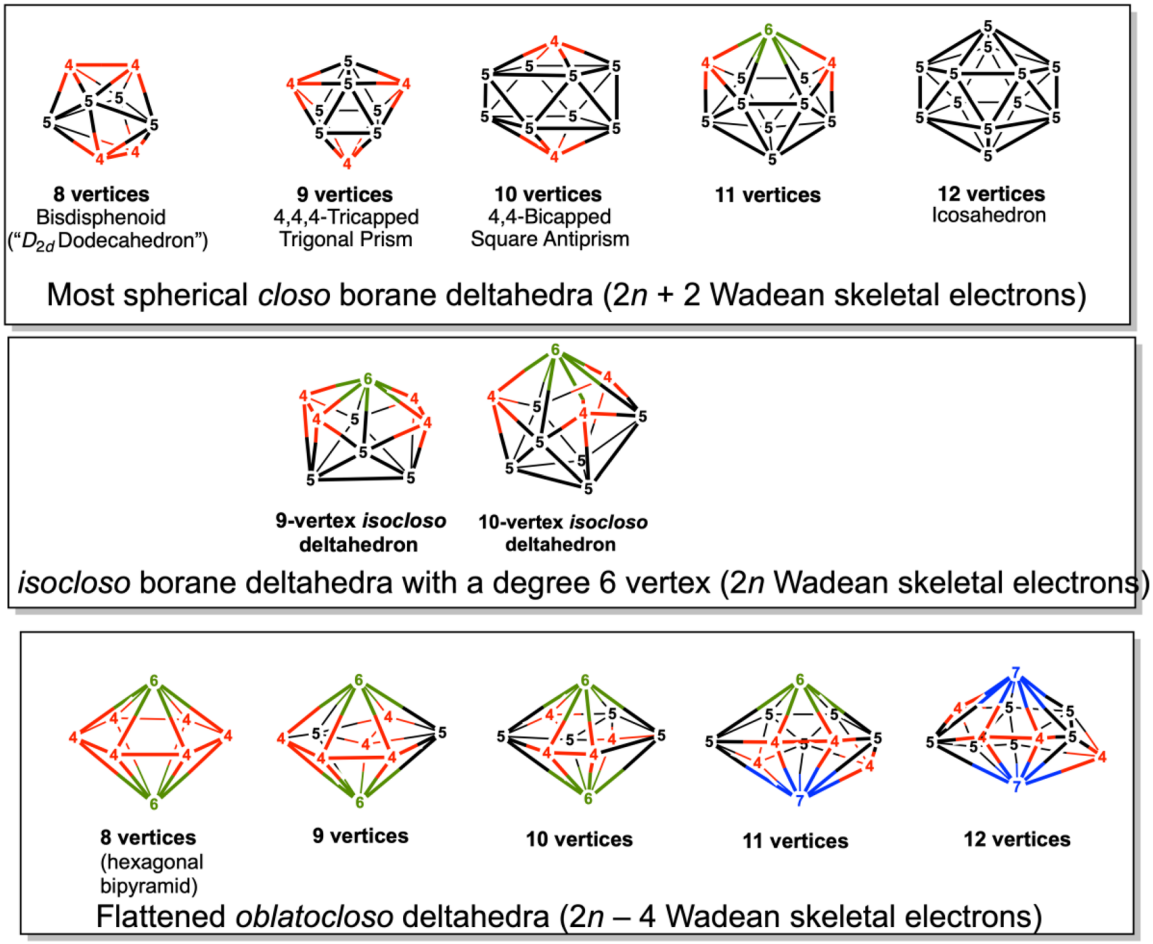

Fig. 1 The *closo*, iso*closo*, and oblato*closo* deltahedra having 8 to 12 vertices. Vertices of degrees 4, 5, 6, and 7 are indicated in red, black, green, and blue, respectively.

systems using platinum group metals of the 4d and 5d transition series as vertex atoms. The Kennedy group identified alternative deltahedra known as iso*closo*[14] or hyper*closo*[15–17] deltahedra for the 9- and 10-vertex systems, particularly the latter (Fig. 1).[18–21] The iso*closo* 9- and 10-vertex deltahedra have a single degree 6 vertex, whereas the corresponding 9- and 10-vertex *closo* deltahedra have exclusively degree 4 and 5 vertices (Fig. 1). The favored skeletal electron count for *n*-vertex iso*closo* metallaboranes was 2*n*, so they were hypoelectronic relative to the 2*n* + 2 skeletal electron count for the corresponding *n*-vertex *closo* metallaboranes. However, O'Neill and Wade[22] showed that the 8- and 9-vertex *closo* deltahedra have non-degenerate molecular orbitals in the frontier regions so that either 2*n* or 2*n* + 2 skeletal electrons could be favored for these systems. This is reflected experimentally in the long-known[23,24] deltahedral boron chlorides B_nCl_n (*n* = 8, 9) as well as the dirhodaboranes $Cp^*_2Rh_2B_{n-2}H_{n-2}$ (Cp^* = η-Me_5C_5) synthesized by Ghosh and co-workers in recent years.[25,26]

A seminal advance in the chemistry of metallaboranes was the discovery of dirhenaboranes $Cp^*_2Re_2B_{n-2}H_{n-2}$ (*n* = 8, 9, 10, 11, 12) by Ghosh, Fehlner, and their coworkers.[27] X-ray crystallography showed that these dirhenaboranes have a non-spherical deltahedral structure approximating an oblate (flattened) ellipsoid in which one of the three primary axes is significantly shorter than the other two (Fig. 1). Because of this characteristic, deltahedra of this type can conveniently be designated as oblato*closo* deltahedra.[28] The only one of these five oblato*closo* deltahedra that is clearly recognizable is the hexagonal bipyramid. In these oblato*closo* deltahedra, the rhenium atoms are degree 6 or 7 vertices located at relatively flat points on the deltahedral surface, whereas the boron atoms are degree 4 or 5 vertices located at relatively high curvature points on the deltahedral surface. Electron bookkeeping using the Wade–Mingos assumption that the Cp*Re vertices use three of the rhenium valence orbitals for skeletal bonding classifies them as more severely hypoelectronic systems with 2*n* − 4 Wadean skeletal electrons. This hypoelectronicity is illusory, however, since a more reasonable chemical bonding scheme considers the rhenium atoms at degree 6 and 7 vertex sites of low local curvature to use five rather than three valence orbitals for skeletal bonding, thereby making them effectively 2*n* + 4 skeletal electron systems.

Several years ago, we gratifyingly showed by density functional theory (DFT) calculations that these unusual experi-

mentally known oblato*closo* $Cp^*_2Re_2B_{n-2}H_{n-2}$ (n = 8, 9, 10, 11, 12) structures (Fig. 1) with the rhenium atoms in approximately antipodal positions are the lowest energy isomers.[29] However, higher energy $Cp^*_2Re_2B_{n-2}H_{n-2}$ isomers were found exhibiting a new structural paradigm, namely that of a *closo* deltahedron having adjacent rhenium atoms with a short rhenium–rhenium distance suggesting a multiple bond. Upon replacement of the two Cp*Re vertices with a single $PnRe_2$ unit (Pn = pentalenyl {$\eta^{5,5}$-C_8H_6}), thereby forcing the two rhenium atoms into adjacent vertices of the Re_2B_{n-2} deltahedron, such *closo* deltahedral structures were found by DFT to be the lowest energy structures.[30]

The synthetic methods used to prepare these dirhenaboranes of considerable structural interest not only involve the rare metal rhenium but also require several steps to prepare the Cp^*ReCl_4 starting material from typical rhenium sources such as perrhenate. Therefore, our subsequent theoretical studies were directed to explore the viability of structures similar to the dirhenaboranes but using the more abundant first-row transition metals. Our first work in this area studied dichromadicarbaboranes of the $Cp_2Cr_2C_2B_{n-4}H_{n-2}$ isoelectronic type with $Cp^*_2Re_2B_{n-2}H_{n-2}$ systems.[31] In addition, Stone and co-workers[32] reported a species formulated as $Cp_2Cr_2C_2B_8H_{10}$ shown by X-ray crystallography to have a central $Cr_2C_2B_8$ icosahedron with adjacent chromium vertices with a short chromium–chromium distance of 2.272 Å. Initially we thought that this short chromium–chromium distance might correspond to the formal quadruple bond required to provide enough skeletal electrons from the chromium atoms to give 26 (=2n + 2 for n = 12) skeletal electrons for a *closo* icosahedral system. However, our conclusion from this study based on the comparison of predicted chromium–chromium distances for various structures with the experimental chromium–chromium distance determined by X-ray crystallography suggested that the species reported by Stone and co-workers has a Cr≡Cr triple bond bridged by two hydrogen atoms, not revealed in their X-ray crystallographic study dating back to the 1980s. In general, this study revealed low-energy oblato*closo* structures $Cp_2Cr_2C_2B_{n-4}H_{n-2}$ similar to those of their isoelectronic rhenium $Cp^*_2Re_2B_{n-2}H_{n-2}$ analogues as well as *closo* and iso*closo* structures with short chromium–chromium distances, suggesting formal quadruple and triple bonds, respectively.

More recently, we used DFT to study $Cp_2Mn_2B_{n-2}H_{n-2}$ systems that are the direct analogues of $Cp_2Re_2B_{n-2}H_{n-2}$ systems for which the oblato*closo* structures are preferred.[33] However, low-energy oblato*closo* structures were not found for dimanganese systems. Instead, the energetically preferred structures for the $Cp_2Mn_2B_{n-2}H_{n-2}$ systems were found to be higher spin state triplet and quintet structures, apparently a consequence of the lower ligand field strength in manganese complexes relative to analogous rhenium complexes. In general, the lowest energy $Cp_2Mn_2B_{n-2}H_{n-2}$ structures were typically found to have a central MnB_{n-1} *closo* deltahedron with one face capped by the second CpMn unit.

Our studies on the $Cp_2Cr_2C_2B_{n-4}H_{n-2}$ systems found a variety of interesting singlet oblato*closo*, iso*closo*, and *closo* structures as low-energy structures. We now report a DFT investigation of the corresponding divanadadicarbaboranes $Cp_2V_2C_2B_{n-4}H_{n-2}$. Unexpectedly, we found that the low-energy vanadadicarbaborane structures are of a totally different type from those of the dichromadicarbaboranes. Thus, the low-energy $Cp_2V_2C_2B_{n-4}H_{n-2}$ structures are seen to resemble those of the dimanganaboranes $Cp_2Mn_2B_{n-2}H_{n-2}$ in exhibiting higher spin state triplet and quintet structures with central VC_2B_{n-3} deltahedra capped by a high-spin CpV unit, even though the $Cp_2V_2C_2B_{n-4}H_{n-2}$ and $Cp_2Mn_2B_{n-2}H_{n-2}$ systems are not isoelectronic. Our results thus show that the two skeletal electron difference resulting in the substitution of vanadium for chromium in the dimetalladicarbaboranes $Cp_2M_2C_2B_{n-4}H_{n-2}$ has a profound effect on the energetically preferred structure types.

2. Theoretical methods

The initial $Cp_2V_2C_2B_{n-4}H_{n-2}$ structures were constructed by systematic substitution of two boron vertices in $B_nH_n^{2-}$ with two CpV units in various n-vertex polyhedral geometries, followed by further substitution of two of the remaining BH vertices by CH vertices. Thus, 337 structures of the 8-vertex $Cp_2V_2C_2B_4H_6$ clusters, 347 structures of the 9-vertex $Cp_2V_2C_2B_5H_7$ clusters, 538 structures of the 10-vertex $Cp_2V_2C_2B_6H_8$ clusters, 407 structures of the 11-vertex $Cp_2V_2C_2B_7H_9$ clusters, and 223 structures of the 12-vertex $Cp_2V_2C_2B_8H_{10}$ clusters were chosen as starting points for the optimizations (see the ESI†).

Full geometry optimizations were carried out on the $Cp_2V_2C_2B_{n-4}H_{n-2}$ systems (n = 8–12) at the B3LYP/6-31G(d) level of theory with all of them optimized, in turn, as neutral singlets, triplets, and quintets. For the singlet structures, the broken symmetry approach was also considered. The lowest-energy structures were then reoptimized at a higher level of theory, namely PBE0/Def2TZVP, and these are the structures presented in the manuscript.[34] The nature of the stationary points after the optimization was checked by calculations of harmonic vibrational frequencies. If significant imaginary frequencies were found, the optimization was continued by following the normal modes corresponding to the imaginary frequencies to ensure that genuine minima were obtained.

All calculations were performed using the Gaussian 09 package[35] with the default settings for the SCF cycles and geometry optimization. The Wiberg bond indices (WBIs) for the V–V interactions in the optimized $Cp_2V_2C_2B_{n-4}H_{n-2}$ structures were obtained from the NBO analysis automatically provided in the Gaussian output.[36] All of the structures reported in this paper have appreciable HOMO–LUMO gaps of 2.59–4.40 eV (see Table S7 in the ESI†).

The $Cp_2V_2C_2B_{n-4}H_{n-2}$ (n = 8 to 12) structures are numbered as **B(*n*−4)C2V2-*x*Y** where n is the total number of polyhedral vertices, x is the relative order of the structure on the energy scale (PBE0/Def2TZVP including zero-point corrections) and Y is the spin state designating singlets, triplets, and quintets as

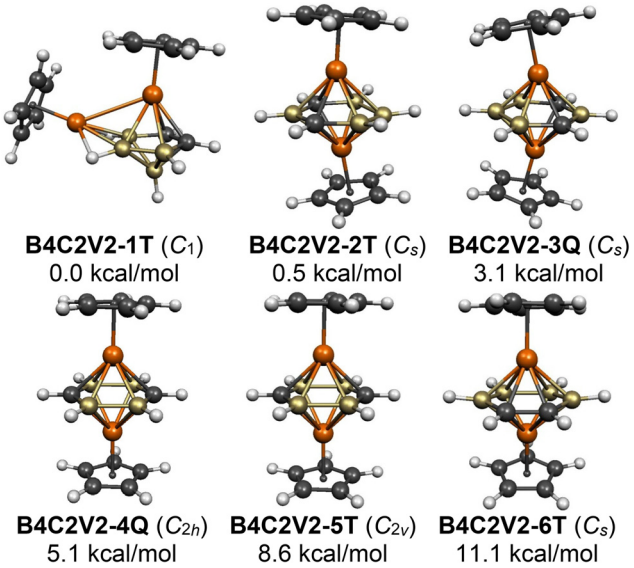

Fig. 2 The lowest energy 8-vertex $Cp_2V_2C_2B_4H_6$ structures.

S, T and Q. The lowest energy optimized structures discussed in this paper are depicted in Fig. 2 through 6. Only the lowest energy and thus potentially chemically significant structures are considered in detail in this paper. More comprehensive lists of structures, including higher energy structures, are given in the ESI.†

3. Results and discussion

3.1. Eight-vertex $Cp_2V_2C_2B_4H_6$ clusters

Six 8-vertex $Cp_2V_2C_2B_4H_6$ structures were found within 11 kcal mol^{-1} of the lowest energy structure **B4C2V2-1T** (Fig. 2 and Table 1). The triplet structure **B4C2V2-1T** has a central VC_2B_4 pentagonal bipyramid in which one face is capped by a CpV moiety with two hydrogen bridges to this vanadium atom from adjacent boron atoms. The spin density on the capping vanadium atom of 3.22 corresponds to the three unpaired electrons of high-spin vanadium(II) in a CpV^+ moiety. This is analogous to the localization of five unpaired electrons in the capping $CpMn^+$ moieties in many of the previously studied dimanganaboranes.[33] The opposing spin density of −1.17 on the other vanadium atom located at one of the apices of the pentagonal bipyramid leads to a net vanadium spin of 2.05, consistent with the triplet spin state of **B4C2V2-1T**.

The other five low-energy $Cp_2V_2C_2B_4H_6$ structures are all hexagonal bipyramids having the vanadium atoms in the axial positions with V–V distances of ~3 Å, suggesting some vanadium–vanadium interaction through the center of the hexagonal bipyramid (Fig. 2 and Table 1). These five structures can thus be considered as 8-vertex oblato*closo* structures (Fig. 1). The **B4C2V2-2T**, **B4C2V2-5T**, and **B4C2V2-6T** structures lying 0.5, 8.6, and 11.1 kcal mol^{-1}, respectively, above **B4C2V2-1T**, are triplet structures with the two carbon atoms located in *meta* (non-adjacent/non-antipodal), *para* (antipodal), and *ortho* (adjacent) positions in the equatorial hexagon, respectively. The quintet $Cp_2V_2C_2B_4H_6$ structures, **B4C2V2-3Q** and **B4C2V2-4Q**, lying 3.1 and 5.1 kcal mol^{-1}, respectively, in energy above **B4C2V2-1T**, are quite similar to the carbon atoms located in the *meta* and *para* positions in the equatorial hexagon, respectively.

3.2. Nine-vertex $Cp_2V_2C_2B_5H_7$ clusters

The potential energy surface for the 9-vertex $Cp_2V_2C_2B_5H_7$ is more complicated than that of $Cp_2V_2C_2B_4H_6$ with 10 structures lying within 11 kcal mol^{-1} of the lowest energy structure **B5C2V2-1Q** (Fig. 3 and Table 2). This quintet structure **B5C2V2-1Q** has a central VC_2B_4 pentagonal bipyramid with the fifth boron atom capping a VB_2 face. The remaining CpV moiety then caps the B_3 face including this capping boron atom with B–H–V bridges from all three boron atoms in the capped face. This degree 3 capping vanadium atom has a spin density of 3.11 corresponding to a high-spin vanadium(II) CpV^+ similar to that in the $Cp_2V_2C_2B_4H_6$ structure **B4C2V2-1T** (Fig. 2 and Table 1).

Three of the 10 lowest energy $Cp_2V_2C_2B_5H_7$ structures, namely the quintets **B5C2V2-2Q**, **B5C2V2-4Q**, and **B5C2V2-5Q** lying 0.9, 3.3, and 6.4 kcal mol^{-1} above **B5C2V2-1Q**, have central $V_2C_2B_5$ 9-vertex iso*closo* deltahedra (Fig. 3 and Table 2). The somewhat higher energy triplet 9-vertex iso*closo* deltahedral structures **B5C2V2-7T**, **B5C2V2-9T**, and **B5C2V2-10T** lie at 7.1, 9.8, and 10.3 kcal mol^{-1}, respectively, above **B5C2V2-1Q**. All six of these $Cp_2V_2C_2B_5H_7$ structures have one of the vanadium atoms located at the unique degree 6 vertex of the 9-vertex iso*closo* deltahedron. Except for **B5C2V2-4Q**, the second vanadium vertex is not adjacent to the degree 6 vertices, leading to long V···V distances of ~3.7 Å with WBIs of

Table 1 The lowest energy $Cp_2V_2C_2B_4H_6$ structures up to 11.5 kcal mol^{-1}. Energies are given in kcal mol^{-1} and distances are given in Å

		Vanadium vertices				Net V	V···V	V···V	
Structure (symmetry)	ΔE	Degree	Spin	Degree	Spin	Spin	Distance	WBI	Polyhedron
B4C2V2-1T (C_1)	0.0	3(2μ-H)	3.22	6	−1.17	2.05	3.24	0.72	Cap pent bipy
B4C2V2-2T (C_s)	0.5	6	2.91	6	−0.85	2.06	2.95	0.53	Hex bipy
B4C2V2-3Q (C_s)	3.1	6	2.45	6	2.42	4.87	3.04	0.25	Hex bipy
B4C2V2-4Q (C_{2h})	5.1	6	2.33	6	2.33	4.66	3.07	0.22	Hex bipy
B4C2V2-5T (C_{2v})	8.6	6	2.07	6	0.54	2.61	2.86	0.39	Hex bipy
B4C2V2-6T (C_s)	11.1	6	2.65	6	−0.24	2.41	3.26	0.40	Hex bipy

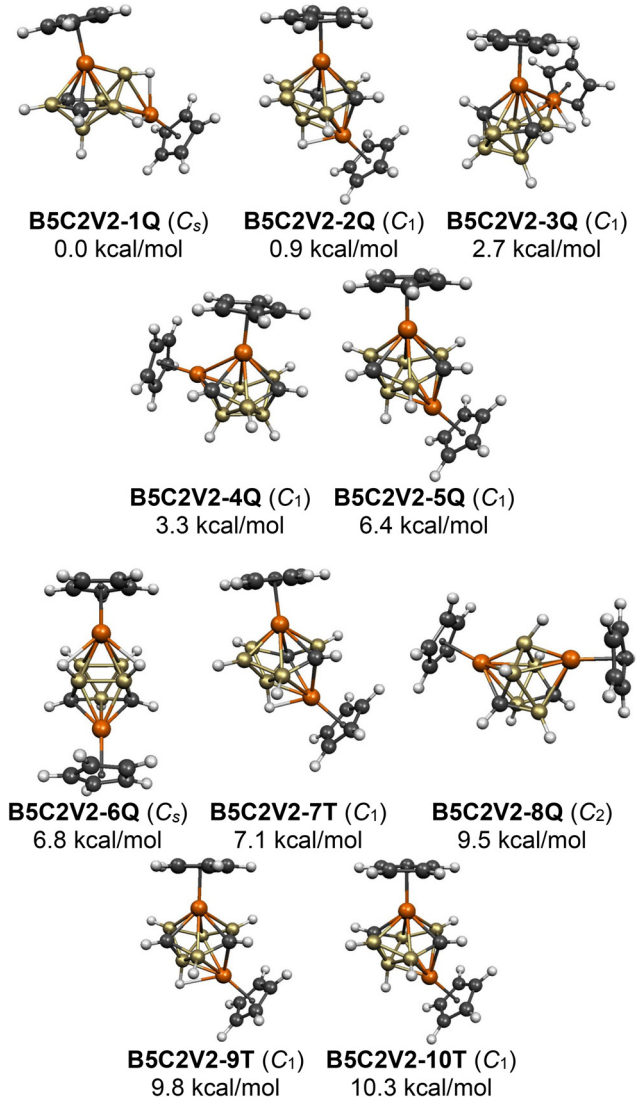

Fig. 3 The lowest energy 9-vertex $Cp_2V_2C_2B_5H_7$ structures.

~0.13 for the quintet structures and ~3.5 Å with somewhat higher WBIs for the triplet structures. The V–V distance in **B5C2V2-4Q** with adjacent vanadium atoms at a distance of 2.78 Å corresponds to a significantly higher WBI of 0.25.

The three remaining $Cp_2V_2C_2B_5H_7$ structures have other central polyhedra (Fig. 3 and Table 2). The quintet structure **B5C2V2-3Q**, lying 2.7 kcal mol^{-1} above **B5C2V2-1Q**, has a central VC_2B_5 bisdisphenoid (the 8-vertex *closo* deltahedron—Fig. 1) with one of its faces capped by a high-spin CpV^+ moiety with a spin density of 3.16 and one B–H–V bridge. The quintet structure **B5C2V2-6Q**, lying 6.8 kcal mol^{-1} above **B5C2V2-1Q**, has a tricapped trigonal prismatic structure (the 9-vertex *closo* deltahedron—Fig. 1) with one vanadium atom at a degree 5 vertex and the other vanadium atom at a degree 4 vertex. The degree 4 vanadium vertex in **B5C2V2-6Q** forms two V–H–B bridges with adjacent boron atoms. Finally, the $V_2C_2B_5$ polyhedron in **B5C2V2-8Q**, lying 9.5 kcal mol^{-1} above **B5C2V2-1Q** in energy, is also a tricapped trigonal prism with the two carbon atoms and a boron atom as degree 4 vertices capping the underlying V_2B_4 trigonal prism.

3.3. Ten-vertex $Cp_2V_2C_2B_6H_8$ clusters

Five 10-vertex $Cp_2V_2C_2B_6H_8$ structures were found within 13 kcal mol^{-1} of the lowest energy structure **B6C2V2-1T** (Fig. 4 and Table 3). The central polyhedron in the triplet structure **B6C2V2-1T** is a 10-vertex iso*closo* polyhedron with one of the

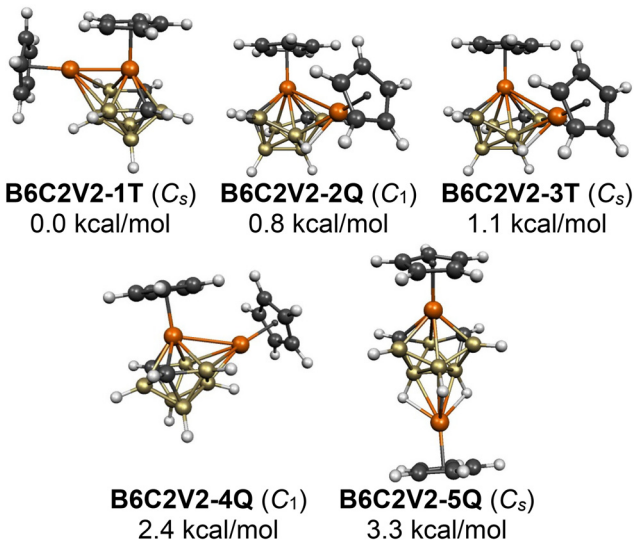

Fig. 4 The lowest energy 10-vertex $Cp_2V_2C_2B_6H_8$ structures.

Table 2 The lowest energy $Cp_2V_2C_2B_5H_7$ structures up to 11 kcal mol^{-1}. Energies are given in kcal mol^{-1} and distances are given in Å

		Vanadium vertices				Net V	V···V	V···V	
Structure (symmetry)	Δ*E*	Degree	Spin	Degree	Spin	Spin	Distance	WBI	Polyhedron
B5C2V2-1Q (C_s)	0.0	3(3μ-H)	3.11	6	1.69	4.80	3.99	0.03	Central pent bipy
B5C2V2-2Q (C_1)	0.9	6	2.28	5	2.32	4.60	3.69	0.14	9-Vertex *isocloso*
B5C2V2-3Q (C_1)	2.7	3(1μ-H)	3.16	6	1.29	4.45	3.07	0.21	Cap bisdisphen
B5C2V2-4Q (C_1)	3.3	4(1μ-H)	2.50	6	2.24	4.74	2.78	0.25	9-Vertex iso*closo*
B5C2V2-5Q (C_1)	6.4	5(1μ-H)	2.37	6	2.29	4.66	3.67	0.12	9-Vertex iso*closo*
B5C2V2-6Q (C_s)	6.8	4(2μ-H)	2.62	5	2.50	5.12	3.91	0.06	Tricap trig prism
B5C2V2-7T (C_1)	7.1	5(1μ-H)	2.37	6	−0.08	2.29	3.50	0.18	9-Vertex iso*closo*
B5C2V2-8Q (C_2)	9.5	5	2.36	5	2.35	4.70	3.84	0.10	Tricap trig prism
B5C2V2-9T (C_1)	9.8	5	2.40	6	−0.09	2.31	3.54	0.15	9-Vertex iso*closo*
B5C2V2-10T (C_1)	10.3	5	2.40	6	−0.07	2.33	3.44	0.19	9-Vertex iso*closo*

Table 3 The lowest energy $Cp_2V_2C_2B_6H_8$ structures up to 13 kcal mol^{-1}. Energies are given in kcal mol^{-1} and distances are given in Å

		Vanadium vertices				Net V	V⋯V	V⋯V	
Structure (symmetry)	ΔE	Degree	Spin	Degree	Spin	Spin	Distance	WBI	Polyhedron
B6C2V2-1T (C_s)	0.0	4	3.09	6	−1.23	1.86	2.53	0.56	10v-iso*closo*
B6C2V2-2Q (C_1)	0.8	3(1μ-H)	3.15	7	1.32	4.47	3.31	0.10	Cap 9v iso*closo*
B6C2V2-3T (C_s)	1.1	3(3μ-H)	3.17	7	−1.25	1.92	3.36	0.11	Cap 9v iso*closo*
B6C2V2-4Q (C_s)	2.4	3(1μ-H)	3.17	7	1.29	4.46	4.01	0.18	Cap 9v iso*closo*
B6C2V2-5Q (C_s)	3.3	3(3μ-H)	3.15	6	1.32	4.47	4.64	0.02	Cap 9v iso*closo*

vanadium atoms at the degree 6 vertex. The short V═V distance of 2.53 Å with a relatively high WBI of 0.56 in **B6C2V2-1T** suggests some type of multiple bond. The second vanadium atom in **B6C2V2-1T** is a degree 4 vertex with a high spin density of 3.09 corresponding to a high-spin vanadium(II) CpV^+ unit similar to that found in a number of the other low-energy $Cp_2V_2C_2B_{n-4}H_{n-2}$ structures.

The remaining four low-energy $Cp_2V_2C_2B_6H_8$ structures, namely **B6C2V2-2Q**, **B6C2V2-3T**, **B6C2V2-4Q**, and **B6C2V2-5Q**, are closely spaced in energy, lying 0.8, 1.1, 2.4, and 3.3 kcal mol^{-1}, respectively, above **B6C2V2-1T**. All four structures have a central 9-vertex iso*closo* VC_2B_6 deltahedron (Fig. 1), in which one of the faces is capped by a high-spin vanadium(II) atom in a CpV^+ unit with a spin density of ~3.15 (Fig. 4 and Table 3). These four nearly isoenergetic structures differ in their spin state and in which of the faces of the 9-vertex iso*closo* deltahedron is capped by the second vanadium atom.

3.4. Eleven-vertex $Cp_2V_2C_2B_7H_9$ clusters

The relevant potential energy surfaces of the 11-vertex $Cp_2V_2C_2B_7H_9$ system (Fig. 5 and Table 4) and the 12-vertex $Cp_2V_2C_2B_8H_{10}$ system are simple compared with the systems with fewer vertices discussed above. Thus the 11-vertex $Cp_2V_2C_2B_7H_9$ system has three structures within 5 kcal mol^{-1} of the lowest energy structure **B7C2V2-1Q**. However, any other isomeric structures lie at least 18 kcal mol^{-1} above **B7C2V2-1Q** (Fig. 5). All three of these structures have a central VC_2B_7 bicapped square antiprism (the 10-vertex *closo* deltahedron—Fig. 1), in which one of the faces is capped by a high-spin CpV^+ unit with a spin density of ~3.15. The capping vanadium atoms form one to three V–H–B bridges to adjacent boron atoms (Table 4). In all three $Cp_2V_2C_2B_7H_9$ structures, the capped face includes one of the degree 4 vertices of the underlying deltahedron.

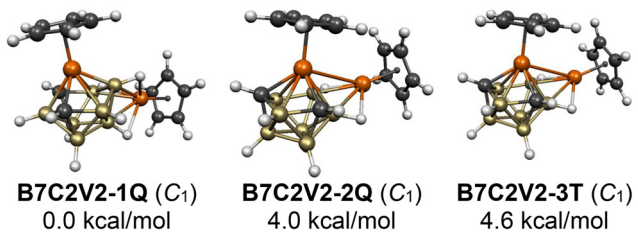

Fig. 5 The lowest energy 11-vertex $Cp_2V_2C_2B_7H_9$ structures.

3.5. Twelve-vertex $Cp_2V_2C_2B_8H_{10}$ clusters

The potential energy surface of the 12-vertex $Cp_2V_2C_2B_8H_{10}$ system is even simpler since the lowest energy structure **B8C2V2-1Q** (Fig. 6) lies ~18 kcal mol^{-1} below the next lowest energy structure, which has a similar geometry but with a triplet rather than quintet spin state. Structure **B8C2V2-1Q** is a capped 11-vertex *closo* deltahedron with one of the vanadium atoms at a degree 6 vertex. The other vanadium atom is the degree 3 capping atom with a spin density of 3.18 corresponding to a high-spin CpV^+ unit. This capping vanadium atom forms three V–H–B bridges with adjacent boron atoms.

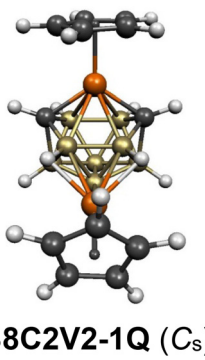

Fig. 6 The lowest energy $Cp_2V_2C_2B_8H_{10}$ structure **B8C2V2-1Q** lying ~18 kcal mol^{-1} in energy below the next lowest energy structure.

Table 4 The lowest energy $Cp_2V_2C_2B_7H_9$ structures up to 18 kcal mol^{-1}. Energies are given in kcal mol^{-1} and distances are given in Å

		Vanadium vertices				Net V	V⋯V	V⋯V	
Structure (symmetry)	ΔE	Degree	Spin	Degree	Spin	Spin	Distance	WBI	Polyhedron
B7C2V2-1Q (C_s)	0.0	3(2μ-H)	3.15	6	1.55	4.70	4.19	0.02	Cap 10v *closo*
B7C2V2-2Q (C_1)	4.0	3(1μ-H)	3.14	6	1.55	4.69	3.32	0.10	Cap 10v *closo*
B7C2V2-3T (C_s)	4.6	3(3μ-H)	3.17	6	−1.35	1.82	3.35	0.11	Cap 10v *closo*

4. Conclusion

In a previous study,[31] the low-energy structures of the dichromadicarbaboranes $Cp_2Cr_2C_2B_{n-4}H_{n-2}$ (n = 8 to 12) were found to be singlet spin state structures with flattened oblato*closo* $Cr_2C_2B_{n-4}$ deltahedra having degree 6 and 7 chromium vertices similar to the lowest energy[29] and experimentally known[27] structures of the isoelectronic dirhenaboranes $Cp_2Re_2B_{n-4}H_{n-2}$. In addition, singlet spherical *closo* deltahedral structures having adjacent chromium vertices with surface chromium–chromium triple or quadruple bonds are found for the dichromadicarbaboranes at accessible energies.

Simple substitution of two vanadium atoms for the two chromium atoms in the dichromadicarbaboranes to give the divanadadicarbaboranes $Cp_2V_2C_2B_{n-4}H_{n-2}$ (n = 8 to 12) leads to very different potential energy surfaces with all of the lowest energy structures being higher spin state triplet and quintet structures rather than singlet structures. A conspicuous feature in many of the low-energy structures is a degree 3 high-spin vanadium(II) CpV^+ moiety capping a face of an (n − 1)-vertex deltahedron with one to three B–H–V bridges to this vanadium atom. In this respect, the divanadadicarbaboranes resemble the dimanganaboranes[33] $Cp_2Mn_2B_{n-2}H_{n-2}$, even though the systems are not isoelectronic. Thus the low-energy dimanganaborane structures are all higher spin triplet and quintet spin state structures with the frequent feature of a similar high-spin $CpMn^+$ moiety capping a face of an (n − 1)-vertex deltahedron with one to three B–H–Mn bridges to the capping manganese atom.

Most of the low-energy 8-vertex divanadadicarbaboranes $Cp_2V_2C_2B_4H_6$ exhibit oblato*closo* structures having a $V_2C_2B_4$ hexagonal bipyramid with the vanadium atoms in antipodal positions at the low-curvature degree 6 vertices. The 9-vertex $Cp_2V_2C_2B_5H_7$ potential energy surface is rather complicated but the 9-vertex iso*closo* deltahedron (Fig. 1) is a key feature of many of the low-energy structures. Most of the low-energy structures for the 10-vertex $Cp_2V_2C_2B_6H_8$ system are also based on a central 9-vertex VC_2B_6 iso*closo* deltahedron but with one of the faces capped by the second vanadium atom in a high-spin vanadium(II) CpV^+ moiety with one to three B–H–V hydrogen bridges to this vanadium atom. The three lowest-energy structures of the 11-vertex $Cp_2V_2C_2B_7H_9$ system by a wide margin all have a central 10-vertex VC_2B_7 *closo* deltahedron, namely the bicapped square antiprism (Fig. 1), in which one of the faces is capped by the second vanadium atom, likewise in a high-spin CpV^+ moiety bridged by one to three hydrogen atoms to the adjacent boron atoms. The lowest energy $Cp_2V_2C_2B_8H_{10}$ structure by a substantial margin of ~18 kcal mol^{-1} has a central 11-vertex *closo* deltahedron capped by a high-spin vanadium vertex with three V–H–B bridges.

Conflicts of interest

The authors declare no competing financial interest.

Data availability

The data are available from the authors upon request.

Acknowledgements

The computational facilities were provided by the Babeș-Bolyai University under project POC/398/1/1/124155 – co-financed by the European Regional Development Fund (ERDF) through the Competitiveness Operational Program for Romania 2014–2020.

References

1 A. S. Weller, Carboranes including their metal complexes, in *Organometallic Chemistry*, ed. M. Green, RSC Publishing, 2002, vol. 30.
2 *Boron Science New Technologies and Applications*, ed. N. S. Hosmane, Taylor and Francis, 2011.
3 *Handbook of Boron Science With Applications in Organometallics, Catalysis, Materials and Medicine*, ed. N. S. Hosmane and R. Eagling, World Scientific, 2018.
4 K. Wade, The structural significance of the number of skeletal bonding electron-pairs in carboranes, the higher boranes and borane anions, and various transition-metal carbonyl cluster compounds, *J. Chem. Soc. D: Chem. Commun.*, 1971, 792–793.
5 D. M. P. Mingos, A general theory for cluster and ring compounds of the main group and transition elements, *Nature Phys. Sci.*, 1972, **236**, 99–102.
6 D. M. P. Mingos, Polyhedral skeletal electron pair approach, *Acc. Chem. Res.*, 1984, **17**, 311–319.
7 R. B. King and D. H. Rouvray, A graph-theoretical interpretation of the bonding topology in polyhedral boranes, carboranes, and metal clusters, *J. Am. Chem. Soc.*, 1977, **99**, 7834–7840.
8 A. J. Stone and M. J. Alderson, A new model of structure and bonding in the boron hydrides, *Inorg. Chem.*, 1982, **21**, 2297–2302.
9 K. P. Callahan and M. F. Hawthorne, Ten years of metallocarboranes, *Adv. Organomet. Chem.*, 1976, **14**, 145–186.
10 R. N. Grimes, The role of metals in borane clusters, *Acc. Chem. Res.*, 1983, **16**, 22–26.
11 S. C. Rasmussen, The 18-electron rule and electron counting in transition metal compounds: theory and application, *ChemTexts*, 2015, **1**, 10.
12 C. A. Tolman, The 16 and 18 electron rule in organometallic chemistry and homogeneous catalysis, *Chem. Soc. Rev.*, 1972, **1**, 337–353.
13 D. P. Craig and G. Doggett, Theoretical basis of the "rare-gas rule", *J. Chem. Soc.*, 1963, 4189.
14 J. D. Kennedy, Structure and bonding in recently isolated metallaboranes, *Inorg. Chem.*, 1986, **25**, 111–112.
15 R. T. Baker, Hyper-*closo* metallaboranes, *Inorg. Chem.*, 1986, **25**, 109–111.

16 R. L. Johnston and D. M. P. Mingos, Molecular orbital calculations relevant to the hyper*closo* vs. iso-*closo* controversy in metallaboranes, *Inorg. Chem.*, 1986, **25**, 3321–3323.
17 R. L. Johnston, D. M. P. Mingos and P. Sherwood, Bonding and electron counting in hyper *closo* metalloboranes and metallocarboranes, *New J. Chem.*, 1991, **15**, 831–841.
18 J. Bould, J. D. Kennedy and M. Thornton-Pett, Ten-vertex metallaborane chemistry. Aspects of the iridadecaborane *closo*→isonido→iso*closo* structural continuum, *J. Chem. Soc., Dalton Trans.*, 1992, 563–576.
19 J. D. Kennedy and B. Štibr, in *Current Topics in the Chemistry of Boron*, ed. G. W. Kabalka, Royal Society of Chemistry, Cambridge, 1994, pp. 285–292.
20 J. D. Kennedy, in *The Borane-Carborane-Carbocation Continuum*, ed. J. Casanova, Wiley, New York, 1998, ch. 3, pp. 85–116.
21 B. Štibr, J. D. Kennedy, E. Drdáková and M. Thornton-Pett, Nine-vertex polyhedral iridamonocarbaborane chemistry. Products of thermolysis of $[(CO)(PPh_3)_2IrCB_7H_8]$ and emerging alternative cluster-geometry patterns, *J. Chem. Soc., Dalton Trans.*, 1994, 229–236.
22 M. E. O'Neill and K. Wade, *Closo* clusters with unusual electron numbers: The significance of frontier orbital degeneracies and bonding characteristics, *J. Mol. Struct.: THEOCHEM*, 1983, **103**, 259–268.
23 J. A. Morrison, Chemistry of the polyhedral boron halides and the diboron tetrahalides, *Chem. Rev.*, 1991, **91**, 35–48.
24 C. Corminboeuf, M. W. Wodrich, R. B. King and P. v. R. Schleyer, Effects of halogen substitution on the properties of eight- and nine-vertex *closo*-boranes, *Dalton Trans.*, 2008, 1745–1751.
25 R. Borthakur, B. Mondal, P. Nandi and S. Ghosh, Hypoelectronic isomeric diiridaboranes $[(Cp^*Ir)_2B_6H_6]$: the "Rule-Breakers"(Cp^* = η5-C_5Me_5), *Chem. Commun.*, 2016, **52**, 3199–3202.
26 D. K. Roy, R. Borthakur, R. Prakash, S. Bhattacharya, R. Jagan and S. Ghosh, Hypoelectronic 8–11-Vertex irida- and rhodaboranes, *Inorg. Chem.*, 2016, **55**, 4764–4770.
27 For a review of much of the relevant chemistry from Fehlner's group, see: T. P. Fehlner, in *Group 13 Chemistry: From Fundamentals to Applications*, ed. P. J. Shapiro and D. A. Atwood, American Chemical Society, Washington, D. C., 2002, pp. 49–67.
28 R. B. King, The oblate deltahedra in dimetallaboranes: geometry and chemical bonding, *Inorg. Chem.*, 2006, **45**, 8211–8216.
29 A. Lupan and R. B. King, Hypoelectronic dirhenaboranes having eight to twelve vertices: internal versus surface rhenium-rhenium bonding, *Inorg. Chem.*, 2012, **51**, 7609–7616.
30 A. Lupan and R. B. King, Dimetallaboranes with polyhedral surface metal-metal multiple bonds: deltahedral dirhenaboranes with pentalenedirhenium vertices, *Organometallics*, 2013, **32**, 4002–4008.
31 S. Jakó, A. Lupan, A.-Z. Kun and R. B. King, Spherical *closo* deltahedra with surface metal-metal multiple bonding versus oblate deltahedra with internal metal-metal bonding in dichromadicarbaborane structures: The nature of Stone's icosahedral dichromadicarbaborane, *Inorg. Chem.*, 2019, **58**, 3825–3837.
32 G. K. Barker, M. R. Godfrey, M. Green, H. E. Parge, F. G. A. Stone and A. J. Welch, Synthesis and molecular structures of nido,-[9-((-C_5H_5)-7,8,9-$C_2NiB_8H_{11}$], *nido*-[9-((-C_5H_5-$\mu_{10,11}$-(Ph_3PAu)-7.8.9-$C_2NiB_8H_{10}$], and *closo*-[1,3-((-C_5H_5)$_2$-1,2,3,4-$CrCCrCB_8H_{10}$]: Evidence for a multiple metal-metal bond in a dimetallacarbaborane, *J. Chem. Soc., Chem. Commun.*, 1983, 277–279.
33 A. Găină-Gardiuta, A. Lupan and R. B. King, Triplet capped deltahedral structures rather than singlet oblato*closo*, structures as energetically favored dimanganaborane structures: A new structural paradigm in hypoelectronic metallaborane chemistry, *Inorg. Chem.*, 2022, **61**, 20793–20803.
34 C. Adamo and V. Barone, Toward reliable density functional methods without adjustable parameters: The PBE0 model, *J. Chem. Phys.*, 1999, **110**, 6158–6170.
35 *Gaussian 09 (Revision A.02)*, Gaussian, Inc., Wallingford, CT, 2009. The complete reference is given in the ESI.†
36 F. Weinhold and C. R. Landis, *Valency and Bonding: A Natural Bond Order Donor-Acceptor Perspective*, Cambridge University Press, Cambridge, England, U. K., 2005, pp. 32–36.